

This discussion paper is/has been under review for the journal *Atmospheric Chemistry and Physics (ACP)*. Please refer to the corresponding final paper in *ACP* if available.

**Fossil CO₂ model
intercomparison**

P. Peylin et al.

Importance of fossil fuel emission uncertainties over Europe for CO₂ modeling: model intercomparison

P. Peylin^{1,8}, S. Houweling^{2,3}, M. C. Krol^{2,3,4}, U. Karstens⁵, C. Rödenbeck⁵,
C. Geels⁶, A. Vermeulen⁷, B. Badawy⁵, C. Aulagnier⁵, T. Pregger⁹, F. Delage¹,
G. Pieterse³, P. Ciais¹, and M. Heimann⁵

¹Laboratoire des Sciences du Climat et de l'Environnement, Gif Sur Yvette, France

²National Institute for Space Research, Utrecht, The Netherlands

³Institute for Marine and Atmospheric Research Utrecht, Utrecht, The Netherlands

⁴Wageningen University and Research, Wageningen, The Netherlands

⁵Max-Planck-Institute for Biogeochemistry, Jena, Germany

Title Page

Abstract

Introduction

Conclusions

References

Tables

Figures

◀

▶

◀

▶

Back

Close

Full Screen / Esc

Printer-friendly Version

Interactive Discussion



**Fossil CO₂ model
intercomparison**

P. Peylin et al.

[Title Page](#)[Abstract](#)[Introduction](#)[Conclusions](#)[References](#)[Tables](#)[Figures](#)[I◀](#)[▶I](#)[◀](#)[▶](#)[Back](#)[Close](#)[Full Screen / Esc](#)[Printer-friendly Version](#)[Interactive Discussion](#)

⁶National Environmental Institute, Roskilde, Denmark

⁷Energy Research Centre of the Netherlands, Petten, The Netherlands

⁸Laboratoire BIOEMCO, THIVERVAL-GRIGNON, France

⁹Institute of Energy Economics and the Rational Use of Energy (IER), Stuttgart, Germany

Received: 2 February 2009 – Accepted: 18 February 2009 – Published: 20 March 2009

Correspondence to: P. Peylin (philippe.peylin@Isce.ipsl.fr)

Published by Copernicus Publications on behalf of the European Geosciences Union.

Abstract

Inverse modeling techniques used to quantify surface carbon fluxes commonly assume that the uncertainty of fossil fuel CO₂ (FFCO₂) emissions is negligible and that intra-annual variations can be neglected. To investigate these assumptions, we analyzed the differences between four fossil fuel emission maps with spatial and temporal differences over Europe and their impact on the model simulated CO₂ concentration. Large temporal flux variations characterize the hourly fields (~40% and ~80% for the seasonal and diurnal cycles, peak-to-peak) and annual country totals differ by 10% on average and up to 40% for some countries (i.e., The Netherlands). These emissions have been prescribed to seven different transport models, resulting in 28 different FFCO₂ concentrations fields.

The modeled FFCO₂ concentration time series at surface sites using time-varying emissions show larger seasonal cycles (+2 ppm at the Hungarian tall tower (HUN)) and smaller diurnal cycles in summer (-1 ppm at HUN) than when using constant emissions. The concentration range spanned by all simulations varies between stations, and is generally larger in winter (up to ~10 ppm peak-to-peak at HUN) than in summer (~5 ppm). The contribution of transport model differences to the simulated concentration std-dev is 2–3 times larger than the contribution of emission differences only, at typical European sites used in global inversions. These contributions to the hourly (monthly) std-dev's amount to ~1.2 (0.8) ppm and ~0.4 (0.3) ppm for transport and emissions, respectively. First comparisons of the modeled concentrations with ¹⁴C-based fossil fuel CO₂ observations show that the large transport differences still hamper a quantitative evaluation/validation of the emission inventories. Changes in the estimated monthly biosphere flux (F_{bio}) over Europe, using two inverse modeling approaches, are relatively small (less than 5%) while changes in annual F_{bio} (up to ~0.15 Gt C/yr) are only slightly smaller than the differences in annual emission totals and around 30% of the mean European ecosystem carbon sink. These results point to an urgent need to improve not only the transport models but also the assumed spatial

Fossil CO₂ model intercomparison

P. Peylin et al.

Title Page

Abstract

Introduction

Conclusions

References

Tables

Figures

◀

▶

◀

▶

Back

Close

Full Screen / Esc

Printer-friendly Version

Interactive Discussion



and temporal distribution of fossil fuel emission maps.

1 Introduction

The combustion of fossil fuel since preindustrial time has caused an increase of the atmospheric CO₂ concentration of about 100 ppm, or 35% of the preindustrial level. Currently about 50% of the annual fossil fuel emissions is absorbed by the oceans and the terrestrial biosphere, which implies that without those sinks the current CO₂ level would approach 500 ppm (Canadell et al., 2007). An important effort in carbon cycle research is to quantify the spatial and temporal characteristics of the land and ocean sinks, and whether or not they will change in the future. A powerful approach to quantify the current sources and sinks of CO₂ is to infer these fluxes from atmospheric concentration measurements, using inverse modeling techniques. In the inversion framework it is commonly assumed that the uncertainty of fossil fuel emissions is negligible compared to the uncertainty of the sought net ocean and land fluxes. Furthermore, it is assumed that intra-annual variations of fossil fuel emissions are negligible compared with the large climatically-driven variations of the biosphere exchanges. These assumptions might not be critical when assessing the annual global carbon budget, except where fossil fuel emissions are important (industrialized regions). This is only partly confirmed by one global inverse modeling study by Gurney et al. (2005), who showed that the neglect of temporal variations in fossil sources caused monthly biases in regional budgets up to 50% during parts of the year.

A recent development is to use atmospheric transport models with increased resolution over specific regions. This approach requires a dense measurement network and high frequency (hourly) sampling, which explains why these activities focus mainly on developed parts of the world, such as Europe (CaroboEurope-IP project) and North America (NACP project) where such measurement networks are in operation. At those higher resolutions, the spatial and temporal distributions of fossil fuel emissions become critical, in particular downwind of industrialized regions where the contribution of

Fossil CO₂ model intercomparison

P. Peylin et al.

Title Page

Abstract

Introduction

Conclusions

References

Tables

Figures

◀

▶

◀

▶

Back

Close

Full Screen / Esc

Printer-friendly Version

Interactive Discussion



**Fossil CO₂ model
intercomparison**

P. Peylin et al.

[Title Page](#)[Abstract](#)[Introduction](#)[Conclusions](#)[References](#)[Tables](#)[Figures](#)[◀](#)[▶](#)[◀](#)[▶](#)[Back](#)[Close](#)[Full Screen / Esc](#)[Printer-friendly Version](#)[Interactive Discussion](#)

fossil fuel emissions to the overall carbon budget is relatively large. Although on the global and annual scale fossil fuel emissions are considered to be accurately known, its distribution within a year and between and within individual countries is still uncertain. The errors associated with the emission inventory estimates at these scales are expected to be rather systematic. However, besides the study of Gurney et al. (2005), almost no quantitative information exists on the importance of fossil fuel space-time distribution uncertainties for regional scale inverse modeling and how these errors compare with transport model uncertainties. If systematic errors in fossil fuel emission maps are indeed significant, this would imply that regional scale CO₂ inversions combined with indirect fossil fuel CO₂ proxies, such as ¹⁴CO₂ measurements, could potentially provide information to further constrain these emissions.

The objectives of this publication are to investigate (i) the magnitude of the uncertainties and biases in fossil fuel CO₂ (FFCO₂) emissions and their intra-annual temporal variations, (ii) their contribution to the uncertainty in simulated CO₂ concentrations, and (iii) their impact on regional scale inverse modeling. We will focus our modeling activities on the European sources and sinks of CO₂. Europe is a particularly interesting test case since the fossil fuel emissions are large (~1.7 Pg C/yr for geographical Europe) compared to the net uptake by the terrestrial biosphere (~0.2 Pg C/yr). This doesn't necessarily imply a worst case scenario, however, since the European fossil fuel emissions are relatively well characterized compared with many other parts of the world.

The intra-annual temporal variations of FFCO₂ emissions are characterized by cyclic variations on the seasonal, weekly and diurnal time scales. All these variations will be taken into account, in contrast with Gurney et al. (2005), who only accounted for seasonal variations. Diurnal emission variations may be important because regional inversions commonly select afternoon measurements to reduce the impact of known errors in the simulation of the diurnal PBL dynamics. Furthermore, errors in the representation of the diurnal cycle affect the simulated diurnal rectifier (Denning et al., 1995), which may cause spurious concentration gradients on larger spatial and tempo-

ral scales.

Our approach to reach the above mentioned objectives is as follows: a set of state of the art FFCO₂ emission inventories is selected, with and without temporal variation as described in Sect. 2.1. These emission inventories define separate FFCO₂ tracers, which are transported forward using a suite of global and regional transport models outlined in Sect. 2.2. Simulated FFCO₂ concentrations are compared at selected European measurement locations, and differences are quantified either across the emission inventories or across the transport models (Sect. 3). The potential of using ¹⁴C to validate fossil fuel CO₂ simulations is investigated based on a comparison with quasi-continuous ¹⁴C-based fossil fuel CO₂ observations, currently available at only few selected sites. Finally, inverse modeling calculations are carried out for one year using the different FFCO₂ emission inventories to investigate the impact of assuming perfect and constant fossil fuel emissions on inversion derived CO₂ source and sink estimates (Sect. 4).

2 Model simulations

2.1 Emission inventories

Model simulations have been carried out for four partially independent fossil fuel CO₂ emission maps (FFCO₂ maps) which differ in their spatial and temporal patterns. The FFCO₂ maps represent different emission inventories as specified in Table 1, for the year 2000.

“T3_annual”

This emission map corresponds to what has been used in the Transcom-3 continuous experiment (Law et al., 2007, <http://www.purdue.edu/transcom/>). The emissions are based on Brenkert (1998) and are kept constant throughout the year. Initially defined

Fossil CO₂ model intercomparison

P. Peylin et al.

Title Page

Abstract

Introduction

Conclusions

References

Tables

Figures

◀

▶

◀

▶

Back

Close

Full Screen / Esc

Printer-friendly Version

Interactive Discussion



for the year 1995, they were rescaled to the emission total for 2000, using the total source from the “EDG_annual” emission inventory described below.

“EDG_annual”

The “EDG_annual” emission map corresponds to the EDGAR FT2000 inventory for year 2000 (van Aardenne et al., 2005), which does not account for intra-annual variations. We only included emission categories accounting for fossil fuel usage and cement production, leaving out all categories accounting for biofuel emissions and emissions from organic waste handling (e.g. from agriculture).

“EDG_hourly”

The “EDG_hourly” emission map is similar to “EDG_annual” except that within Europe it has been convolved with diurnal, weekly and seasonal variations provided by EMEP (Vestreng et al., 2005). EMEP provides temporal anthropogenic emission variations for Europe per source category and for various chemical compounds. The seasonal variations are specified per country. For the daily and weekly variations only average time profiles were available which have been applied uniformly over Europe and throughout the year. As EMEP’s main priority is the forecast of pollution events, their emission inventories do not explicitly address CO₂. To circumvent this problem the temporal profiles of the following tracers have been used for FFCO₂: CO for traffic and SO₂ for industrial sources, power supply, and residential heating. These temporal profiles have been applied to the “EDG_annual” map, after translation of the EMEP source categories (SNAP level 1) to the EDGAR grid.

“IER_hourly”

The “IER_hourly” emission map has been derived from the European emission inventory compiled by IER (Institut für Energiewirtschaft und Rationelle Energieanwendung) for the year 2000 (Pregger et al., 2007) at a relatively high spatial resolution of up

Fossil CO₂ model intercomparison

P. Peylin et al.

Title Page

Abstract

Introduction

Conclusions

References

Tables

Figures

◀

▶

◀

▶

Back

Close

Full Screen / Esc

Printer-friendly Version

Interactive Discussion



to $10 \times 10 \text{ km}^2$ over Germany, including diurnal, weekly and seasonal variations specified by country and time of the year for Germany. “EDG_annual” emissions (without temporal variations) were used to complement the “IER_hourly” emissions outside a European domain including western countries up to the black sea (excluding Russia).

The methodology that has been used to construct the “IER_hourly” emission inventory can be briefly summarized as follows (for more details see Pregger et al., 2007): The IER emission model derives FFCO₂ emissions at high temporal and spatial resolution starting from of a database of annual emissions per country. These annual data are taken from the national reports to the United Nations Framework Convention on Climate Change (UNFCCC) for the year 2000. However, UNFCCC emissions for 2001 have been used in case emission reporting for 2000 were unavailable. In the IER model the national emissions are distributed over administrative units using statistical information, such as population density. Subsequently, the emissions are allocated at higher resolution accounting for point, line and area sources, using a geographic information system (GIS). Emissions are distributed in time according to process specific activity maps, accounting for temporal source variations on the diurnal, weekly and seasonal time scale. These temporal source variations represent, for example, traffic rush hours, the reduced power demand in weekends, domestic heating in winter, and air conditioning in summer. Temporal emission variations of some sources, such as domestic heating, depend on regional variations in climatic conditions. Note that the IER product uses more detailed and calibrated databases for Germany than for the rest of Europe and accounts for temperature dependencies in Germany only (based on measured temperatures).

Figure 1 shows a map of the annual European “IER_hourly” FFCO₂ emissions. The IER source has been interpolated to $0.5^\circ \times 0.5^\circ$ (large squares on the eastern part correspond to the “EDG_annual” emission at $1^\circ \times 1^\circ$). Large emissions associated to industrial areas and big cities are well represented by this map. Note that the emissions over Germany show the highest level of detail, owing to the fact that much information was available to IER for this country.

**Fossil CO₂ model
intercomparison**

P. Peylin et al.

[Title Page](#)[Abstract](#)[Introduction](#)[Conclusions](#)[References](#)[Tables](#)[Figures](#)[◀](#)[▶](#)[◀](#)[▶](#)[Back](#)[Close](#)[Full Screen / Esc](#)[Printer-friendly Version](#)[Interactive Discussion](#)

Comparison of the different emissions maps

Table 2 presents a comparison of annual FFCO₂ emissions for selected European countries and geographical Europe for the “EDG_annual” and “IER_hourly” inventories discussed above and the data reported by Marland et al. (2006). The latter is only used for further verification of country level FFCO₂ emissions. These estimates include emissions from all fossil sources except international shipping and air traffic at cruise altitude (landing and take off cycles are included) and cement production. The comparison indicates that the difference between the national totals is generally around 10%. However, for some countries substantially larger differences are found, such as for the Netherlands, for which the difference between the estimates by EDGAR FT2000 and Marland et al. (2006) is 38%. Similar differences are found for Norway (57%), and Bulgaria (44%). These differences are likely explained by inconsistencies, such as the exact definition of source classes, data gaps, etc. These inconsistencies are difficult to trace without support of inventory experts. In a recent study, Ciais et al. (2008) specifically analyzes the magnitude, trends, and uncertainties in FFCO₂ emission for EU-25, and show greater consistency between the different estimates (around 10%) when differences in system boundaries (e.g. counting or not bunker fuels, non-energy products) are taken into account. However, when FFCO₂ inventories are used by atmospheric modelers it is commonly assumed that they provide a systematic coverage of all fossil CO₂ sources, and that the reported uncertainties represent any deviations from that ideal situation. The accuracy of annual FFCO₂ emissions is therefore often assumed to be much better than 10% (see for example Rödenbeck et al., 2003; Baker et al., 2006; Bousquet et al., 2000). Our inventory comparison for Europe suggests that the differences can be substantially larger at the country scale (see also spatial differences between “IER_hourly” and “EDG_hourly” maps, Fig. S1, supplementary material: <http://www.atmos-chem-phys-discuss.net/9/7457/2009/acpd-9-7457-2009-supplement.pdf>). These differences give rise to what we refer to as “apparent uncertainty”, which is typically substantially larger than the ex-

Fossil CO₂ model intercomparison

P. Peylin et al.

Title Page

Abstract

Introduction

Conclusions

References

Tables

Figures

◀

▶

◀

▶

Back

Close

Full Screen / Esc

Printer-friendly Version

Interactive Discussion



pected intrinsic uncertainty of the underlying data (like for example energy statistics). The differences are likely explained by numerous possible inconsistencies arising from double counting,... In the end, however, the totals are most critical to atmospheric modelers and therefore the “apparent uncertainty” is critical when comparing models to atmospheric measurements, even though the numbers may be judged as unrealistically large by inventory experts.

Figure 2 shows a comparison of FFCO₂ temporal patterns in the emissions for selected countries. Sizeable emission variations are found, related, in particular, to the seasonal cycle (~40% peak-to-peak) and the diurnal cycle (~80% peak-to-peak). The seasonal variations provided by EMEP (as used in “EDG_hourly”) are generally larger than those of IER. As expected, the seasonal emission variation in the Mediterranean countries is less than in more northern countries owing to the mild Mediterranean climate in winter. This is illustrated by the difference between Italy and Germany in Fig. 2. This difference is more prominent for IER than for EMEP. Integrated over Europe the seasonal emission variations of IER and EMEP are in relatively close agreement, although slightly smaller for IER. Note that the relative good agreement is at least partly explained by a substantial contribution of Eastern Europe, where EDGAR FT2000 replaces missing IER estimates. In “EDG_hourly” and “IER_hourly” emissions the diurnal variation is larger than the weekly or seasonal variations all year long. The diurnal pattern of the EMEP emissions is less variable across different countries because the EMEP diurnal cycles do not include country specific information. For Germany, the IER emission variations are about 50% larger than those of EMEP in July, and only slightly larger in January. The morning and afternoon emission maxima are mainly determined by the peak in traffic rush hours. The relative size of these maxima shows slight differences between IER and EMEP. Figure 2 also shows the weekly emission variations in July and January. Smaller emissions (around 15%) occur during the weekend than during the rest of the week in both “EDG_hourly” and “IER_hourly” emissions. EMEP and IER weekly variations are in reasonable agreement, except for Germany where EMEP shows about 50% less variation than IER. This suggests that the weekly emission vari-

**Fossil CO₂ model
intercomparison**

P. Peylin et al.

[Title Page](#)[Abstract](#)[Introduction](#)[Conclusions](#)[References](#)[Tables](#)[Figures](#)[I◀](#)[▶I](#)[◀](#)[▶](#)[Back](#)[Close](#)[Full Screen / Esc](#)[Printer-friendly Version](#)[Interactive Discussion](#)

ations in other countries might also be underestimated by EMEP, since the IER treatment of Germany is most realistic. All these differences are also illustrated for France and Spain in the supplementary material: <http://www.atmos-chem-phys-discuss.net/9/7457/2009/acpd-9-7457-2009-supplement.pdf> (Fig. S2).

In summary, it can be concluded that the European fossil fuel emissions show significant temporal variation on various time scales ($\sim 80\%$ on diurnal, $\sim 40\%$ on seasonal, and $\sim 15\%$ on weekly, peak-to-peak). Furthermore, these variations do not seem to be well quantified given the substantial differences between the estimates provided by EMEP and IER. However, the important question is whether these variations give rise to significant variations in atmospheric FFCO₂ sampled at surface stations. This question will be investigated in the following sections.

2.2 Transport model simulations

The fossil fuel emission maps defined in Sect. 2.1 were prescribed as separate FFCO₂ tracers to 7 transport models (see Table 3). Their horizontal resolutions vary between several square degrees (lat \times lon) for the global models (LMDZ, TM3) to $0.5^\circ \times 0.5^\circ$ for the regional models, which only cover the European domain (DEHM, REMO, CHIMERE). TM5 reaches the highest resolution among the global models, because it is zoomed over Europe at $1^\circ \times 1^\circ$. CHIMERE slightly differs from the two other regional models, DEHM and REMO, as it only models the lower troposphere (up to 500 hPa) with a high vertical resolution (20 levels). COMET is a Lagrangian model in which the air mass trajectories are calculated from 3-hourly ECMWF meteorological fields at $1^\circ \times 1^\circ$ horizontal resolution. Two vertical levels are considered in COMET representing the planetary boundary layer and the free troposphere. Note, that COMET was primarily designed to observational points that are in the mixed PBL. The vertical model resolution near the surface varies substantially between the models. The depth of the first layer ranges from 150 m in LMDZ/TM3 to nearly 30 m in REMO/CHIMERE. More detailed model descriptions can be found in Geels et al. (2007) and Law et al. (2007).

Model simulations were performed for 3 years covering the period 2000–2002 (fol-

Fossil CO₂ model intercomparison

P. Peylin et al.

Title Page

Abstract

Introduction

Conclusions

References

Tables

Figures

◀

▶

◀

▶

Back

Close

Full Screen / Esc

Printer-friendly Version

Interactive Discussion



lowing the Transcom-3 experiment), using analysed meteorology. The model were initialized at 0 ppm and the first two years are only used for spin-up. In the last year, concentrations are extracted at the same measurement sites used in the Transcom-3 model intercomparison and at hourly temporal resolution for all models (Law et al., 2007). Hourly fields from the TM3 (or LMDz) model were used as lateral boundary condition for the regional models, DEHM and REMO (or CHIMERE) and TM5 results were used as background information for COMET. Note finally, that nearly all models employ the ECMWF wind fields, except TM3 that uses NCEP winds.

2.3 Description of the inversions set-up

Inverse modeling calculations were performed to investigate the impact of the differences between fossil fuel inventories on the net exchange of carbon by the European terrestrial biosphere, inferred as a “residual”. Recall that in conventional inversions which neglect uncertainties of fossil fuel emissions the actual errors in the a priori fossil fuel map are projected on the a posteriori derived terrestrial biosphere fluxes. The aim of our inverse modeling calculations is to quantify this error. Although the accuracy of current inversions is known to be primarily limited by the sparseness of the atmospheric network, and by unknown biases in transport models (Gurney et al., 2002; Stephens et al., 2007), systematic errors in fossil fuel space-time distribution might also turn out to be important.

We conducted a series of inversions with two transport models (TM3 and LMDz) out of the seven described above. Currently both inversions solve for CO₂ surface fluxes at the spatial resolution of the model grid, given certain assumptions on their prior error covariance matrix. The inverse set-ups follow from the study of Peylin et al. (2005) and Rödenbeck et al. (2003) for LMDZ and TM3, respectively. Both systems solve for the natural component of the terrestrial fluxes and for the ocean fluxes using atmospheric concentration measurements, atmospheric transport information, and prior information (including estimated a priori errors on the fluxes). The fossil fuel emissions are prescribed to the inversion, using either of the four maps described in Sect. 2.1. The

Fossil CO₂ model intercomparison

P. Peylin et al.

Title Page

Abstract

Introduction

Conclusions

References

Tables

Figures

◀

▶

◀

▶

Back

Close

Full Screen / Esc

Printer-friendly Version

Interactive Discussion



**Fossil CO₂ model
intercomparison**

P. Peylin et al.

[Title Page](#)[Abstract](#)[Introduction](#)[Conclusions](#)[References](#)[Tables](#)[Figures](#)[◀](#)[▶](#)[◀](#)[▶](#)[Back](#)[Close](#)[Full Screen / Esc](#)[Printer-friendly Version](#)[Interactive Discussion](#)

two systems are largely independent regarding their treatment of prior information, but adopt a similar selection of atmospheric stations (see Table 4 for details). The inversions are performed for the period 2000–2002, but we will only discuss the results for 2001, avoiding end effects (as caused both by the initial condition and the time lagged response of the fluxes at the stations).

For each model, we performed four inversions using successively the four different fossil fuel emission maps. In each case, only the land and ocean “residual” fluxes are optimized, while the fossil fuel component and its space-time distribution is assumed perfect and thus kept fixed. In a perfectly constrained inverse problem, i.e. with all fluxes being independently constrained by atmospheric measurements, the differences between the inverted biosphere carbon fluxes would correspond to the differences in the input fossil fuel emissions. However, because of the under-constrained nature of current inversions (i.e., only few observations for a large number of unknown fluxes) the impact of fossil fuel differences might be significantly different, both spatially and temporally. These differences will also spread over adjacent poorly constrained regions, including the oceans. We will thus compare the posterior fluxes (mainly over Europe) with the aim to investigate the sensitivity of the calculated biosphere flux to fossil fuel apparent uncertainties and the neglect of time variations in the prior fossil fuel emissions. The use of two different inverse approaches is important to determine the sensitivities of the FFCO₂ induced emission biases to the choice of inversion procedure.

3 Results: forward modelling

3.1 FFCO₂ Concentration time series

CO₂ concentration time series were simulated for all European measurements sites (see site location at <http://www.carboeurope.org/>). For the sake of brevity, the discussion in this subsection is illustrated with the results for one station, the Hegyhatsal tall

tower (115 m) in Hungary (referred to as “HUN”). Additional results at a second site can be found in the supplementary material (<http://www.atmos-chem-phys-discuss.net/9/7457/2009/acpd-9-7457-2009-supplement.pdf>): Schauinsland (SCH), a mountain station in Germany that is usually incorporated in inversions. We restricted ourself to these two sites as they can be considered representative of several European stations. To deal with the large number of factorial simulations, 7 transport models×4 FFCO₂ emission maps, we reduce the number of time series by displaying means across models and means across emissions. With these two averages, one can compare the effect of emission pattern differences versus transport model differences on the simulated concentrations. We will also discuss the difference between the “_hourly” and “_annual” tracers to illustrate the effect of temporal variations in fossil fuel emissions.

Seasonal cycle

Figure 3 (top) displays the daily mean FFCO₂ concentrations averaged across all models for each emission map at HUN. Like in most inversion set-ups, we selected daytime values (average over 10:00 to 17:00 LT), because existing transport models are known to have difficulties in simulating the stability of the nocturnal planetary boundary layer (PBL) (Geels et al., 2007). The simulated time series show large synoptic variations, up to 5 ppm, superimposed on a seasonal cycle of roughly the same size and a trend of few ppm/yr due to the accumulation of emitted FFCO₂. These features are common to all stations (Fig. S3, supplementary material: <http://www.atmos-chem-phys-discuss.net/9/7457/2009/acpd-9-7457-2009-supplement.pdf>), but the amplitude of the synoptic events and the seasonal cycle varies depending on the location of the site to major industrialized regions.

All tracers show a seasonal cycle, which in the case of constant emissions reflects seasonal changes in the atmospheric transport, especially stronger mixing during summer than during winter over Europe. At HUN, the phase and amplitude of the synoptic events are rather similar for all tracers, which indicates that the variation of atmospheric transport (wind direction, vertical mixing,...) is the dominant factor causing day to day

Fossil CO₂ model intercomparison

P. Peylin et al.

Title Page

Abstract

Introduction

Conclusions

References

Tables

Figures

◀

▶

◀

▶

Back

Close

Full Screen / Esc

Printer-friendly Version

Interactive Discussion



variations of FFCO₂ at this site. Note that the observed amplitude of the synoptic CO₂ variations at HUN is roughly two times larger than the one obtained using FFCO₂ only, confirming that an accurate representation of fossil fuel emissions is essential to understand the observed day to day variations in atmospheric CO₂ concentrations at HUN.

Figure 3 (bottom) shows similar time series but for the average across all emission maps for each transport model. Like in the previous plot, the seasonal and synoptic patterns are also visible but with much less agreement regarding both the amplitude and the timing of the synoptic events. On average the amplitude of the synoptic events is larger for the mesoscale models (REMO, DEHM, CHIMERE and COMET) and TM5 (zoomed model) than for the coarse global models (TM3 and LMDz) and the differences between models are largest in winter. Overall, the transport model spread dominates over the spread induced by the four different fossil fuel emissions. Similar results are found at all European stations, (see for instance, SCH, Fig. S3, supplementary material: <http://www.atmos-chem-phys-discuss.net/9/7457/2009/acpd-9-7457-2009-supplement.pdf>). A quantitative estimate of the spread induced by differences in transport versus the spread induced by differences in the emission maps is made in Sect. 5.

In order to investigate the effect of neglecting temporal variations of fossil fuel emission, we present the differences in FFCO₂ simulated concentration between “EDG_hourly” and “EDG_annual” (Fig. 4 top) and between “IER_hourly” and “EDG_annual” (Fig. 4 bottom) emissions at HUN, for the seven transport models. The difference between the two Edgar emissions (recall that they differ only temporally) shows a marked seasonality for all transport models (less pronounced for COMET) with positive values in winter (up to 3 ppm) and slightly negative values in summer (up to -1 ppm). This difference combines (i) the seasonality of the “EDG_hourly” source with more emissions in winter due to larger heating sources (~50%) and less in summer compared to the constant “EDG_annual” source (Sect. 2.1), and (ii) the seasonality of the atmospheric vertical mixing with the strongest mixing during summer time. Both

**Fossil CO₂ model
intercomparison**

P. Peylin et al.

Title Page

Abstract

Introduction

Conclusions

References

Tables

Figures

◀

▶

◀

▶

Back

Close

Full Screen / Esc

Printer-friendly Version

Interactive Discussion



**Fossil CO₂ model
intercomparison**

P. Peylin et al.

[Title Page](#)[Abstract](#)[Introduction](#)[Conclusions](#)[References](#)[Tables](#)[Figures](#)[◀](#)[▶](#)[◀](#)[▶](#)[Back](#)[Close](#)[Full Screen / Esc](#)[Printer-friendly Version](#)[Interactive Discussion](#)

effects act in the same direction and produce similar results at most stations (SCH station, Fig. S4, supplementary material). However, the amplitude of this seasonal variation ranges from ± 0.5 ppm at remote stations like Pallas in Finland up to ± 5 ppm at stations close to industrial areas (i.e., the Cabauw tower in the Netherlands). The covariance between seasonal variations in emissions and transport contributes by about 1 ppm to the “seasonal rectifier effect” described for CO₂ by Keeling et al. (1989). However, the spatial distribution of the seasonal rectifier from the biosphere is different than that of fossil fuel emissions and more pronounced over Siberia and Canada. Note that the few large negative values for “EDG_hourly” minus “EDG_annual” in winter simulated by COMET (Fig. 4) are probably linked to difficulties in reproducing measurements outside the PBL in this Lagrangian model.

The concentration differences between “IER_hourly” and “EDG_annual” emission also show a significant seasonality but with more complicated temporal patterns depending on the site and the transport model. In this case the spatial differences between the two emission maps (Sect. 2.1) also contribute to the FFCO₂ concentration differences. Overall, the spatial differences appear to be as important as the effect of neglecting the temporal variations in the emissions.

Diurnal cycle in summer

Figure 5 (top) displays the hourly concentrations averaged across all transport models for each tracer at HUN for one week in July. A large diurnal cycle of up to 2 ppm is observed, with larger concentrations during nighttime than during daytime. For the constant emission fields (“T3_annual” and “EDG_annual”), the simulated diurnal variations are fully explained by diurnal variations in the PBL height, which lead to increased FFCO₂ concentrations during nighttime compared to daytime. For the time varying fluxes, increased fossil emissions during daytime oppose this effect reducing the diurnal variations. Overall, accounting for time variations in fossil fuel emissions decreases the diurnal cycle in the simulated summer concentrations by up to 1–2 ppm depending on the station. Note also that there are less differences be-

**Fossil CO₂ model
intercomparison**

P. Peylin et al.

[Title Page](#)[Abstract](#)[Introduction](#)[Conclusions](#)[References](#)[Tables](#)[Figures](#)[I◀](#)[▶I](#)[◀](#)[▶](#)[Back](#)[Close](#)[Full Screen / Esc](#)[Printer-friendly Version](#)[Interactive Discussion](#)

tween the four tracers during daytime than during nighttime because of stronger atmospheric mixing and dilution of the PBL with the free troposphere. Similar results are seen at all stations close to source regions. At remote stations or mountain stations (SCH, Fig. S5, supplementary material: <http://www.atmos-chem-phys-discuss.net/9/7457/2009/acpd-9-7457-2009-supplement.pdf>) the time series display almost no diurnal cycle (or even a slight reverse cycle at mountain sites because stations may reside in the free troposphere at night). The synoptic variations become the dominant mode of short-term variability and the cause of the differences between the fossil fuel simulations.

Figure 3 (bottom) shows similar time series as discussed above but now for the average across all tracers for each transport model. The scatter between the different transport models is much larger, with model to model differences up to 6 ppm and a standard deviation of 0.92 ppm for the selected period (compared with 0.48 ppm for the spread induced by the different emission maps). Some models, like TM5 (and partly COMET) have a large diurnal cycle with elevated FFCO₂ concentrations at night compared to daytime (amplitude of nearly 5 ppm), while TM3 and LMDZ produce much smoother diurnal variations (around 2 ppm). Overall, the scatter appears to be large at all stations (Fig. S5, supplementary material) but with complicated temporal patterns. The exact shape of the diurnal cycle varies between models and the maximum or minimum concentrations occur at different times of the day.

Diurnal cycle in winter

We now investigate the hourly variations for one week in January (Fig. 6, top and bottom). Unlike in summer, no clear diurnal cycle is observed at HUN and synoptic events appear to be the dominant source of FFCO₂ variability. If we consider the average across transport models (Fig. 6, top), the two non-time-varying emission maps lead to similar concentration variations (differences less than 2 ppm) while the “IER_hourly” and “EDG_hourly” simulations differ by up to 4 ppm. Although these differences are caused by both spatial and temporal differences between the emission

maps (Sect. 2.1), temporal source variations are important as indicated by the fact that the differences between “EDG_hourly” and “EDG_annual” can reach 4 ppm for a particular day in winter (Fig. 6, top).

If we now consider the average across emission maps, we obtain a much larger spread ($\sigma=3.20$ ppm, Fig. 6, bottom) compared to the spread induced by differences in emission maps ($\sigma=1.05$ ppm, Fig. 6, top). No clear coherent variations can be discerned between the models at the daily time scale, unlike in summer (see above). The model spread clearly dominates the FFCO₂ concentration variability. Synoptic events are clearly visible but their amplitudes strongly differ between models with smooth concentration variations in TM3/LMDZ (2 ppm) and large variations in TM5/DEHM/COMET (more than 10 ppm). Similar results are found for most of the European sites (SCH, Fig. S6, supplementary material: <http://www.atmos-chem-phys-discuss.net/9/7457/2009/acpd-9-7457-2009-supplement.pdf>).

3.2 Surface concentration fields

In order to further analyze the differences between transport models and emission maps, we compare horizontal distributions of monthly mean mixing ratios at the surface for the full European domain sampled at 12:00 local time for January and July. For this purpose we re-gridded the Eulerian model results (LMDZ, REMO, DEHM, TM3 and TM5) for all tracers on a common resolution of 0.1×0.1 degree over Europe. In order to account for differences in vertical resolution between these models, we calculated the mean mixing ratio in a layer between the surface and ~150 m. Figure 7 displays the concentration fields averaged over simulations of the four emission maps, for January and July, for REMO and LMDZ which approximately span the range of available model resolutions.

First of all, it is clear that the REMO model resolves the spatial gradients caused by the FFCO₂ emissions much better. Individual cities are resolved (i.e., Madrid, Paris, London) and orography is clearly visible. In summer, FFCO₂ hot spots are less pronounced due to enhanced vertical mixing during daytime. The coarser resolution LMDZ

Fossil CO₂ model intercomparison

P. Peylin et al.

Title Page

Abstract

Introduction

Conclusions

References

Tables

Figures

◀

▶

◀

▶

Back

Close

Full Screen / Esc

Printer-friendly Version

Interactive Discussion



**Fossil CO₂ model
intercomparison**

P. Peylin et al.

[Title Page](#)[Abstract](#)[Introduction](#)[Conclusions](#)[References](#)[Tables](#)[Figures](#)[◀](#)[▶](#)[◀](#)[▶](#)[Back](#)[Close](#)[Full Screen / Esc](#)[Printer-friendly Version](#)[Interactive Discussion](#)

model resolves only the main emission regions over North Western Europe and North Italy. The two models agree on a larger trapping of FFCO₂ in the PBL in winter. Compared to the emission map (Fig. 1), the region of maximum FFCO₂ concentrations is shifted Eastwards following the mean air mass flow and this feature is most pronounced in LMDZ. These results confirm the results of previous studies pointing to the preferential export pathways of pollutants within the PBL over continents (Stohl et al., 2002).

To explain the model differences, two effects can be distinguished. First, coarser models represent the FFCO₂ emission at coarser resolution, thereby losing their ability to resolve individual cities. Secondly, higher resolution models better resolve the effects of mountains and land-sea transitions on winds and vertical mixing. To separate the influence of model resolution on emissions and transport, the TM5 model results (at 1 × 1 degree horizontal resolution) were compared to results that were obtained with the same model but with the emission resolution coarsened to the LMDZ resolution. The use of coarsened FFCO₂ emissions in TM5 already explains some of the differences between TM5 and LMDZ, as shown in Fig. 8. For instance, the distinct FFCO₂ concentration maxima over the Netherlands and UK is lost when TM5 uses the coarser emissions. Other differences, like the stronger wintertime maximum over Northern Italy are not explained by the resolution of the applied emission field. Also, the concentration minimum over the Alps in TM5 almost disappears when coarse-resolution emissions are used. In conclusion, the higher spatial resolution of the emissions explains some, but not all of the differences observed between the various models. Depending on the position of a particular measurement station with respect to the grid used by the individual models, these resolution effects also explain part of the model-to-model differences discussed in Sect. 3.1.

3.3 Comparison with FFCO₂ based on ¹⁴CO₂ observations

Monitoring of fossil fuel CO₂ is in principle possible with radiocarbon (¹⁴CO₂) measurements in the PBL over the continent (Levin et al., 2003). Spatial (or tempo-

**Fossil CO₂ model
intercomparison**

P. Peylin et al.

Title Page

Abstract

Introduction

Conclusions

References

Tables

Figures

◀

▶

◀

▶

Back

Close

Full Screen / Esc

Printer-friendly Version

Interactive Discussion



ral) gradients of $^{14}\text{CO}_2$ reflect the excess fossil fuel CO_2 that has been released in the air mass, given that fossil fuel CO_2 is free of ^{14}C . The current European network of stations with quasi-continuous time series of two-weekly or monthly-integrated $^{14}\text{CO}_2$ consists of seven stations, located in remote as well as in more polluted areas.

5 Monthly-integrated FFCO₂ concentrations from all model simulations are compared with $^{14}\text{CO}_2$ -based fossil fuel CO_2 observations for the year 2002. Figure 9 presents the results for the mountain station Schauinsland (SCH), which is often incorporated in inversions, but additional results for the urban site Heidelberg (HEI) are provided in the supplementary material: <http://www.atmos-chem-phys-discuss.net/9/7457/2009/acpd-9-7457-2009-supplement.pdf> (Fig. S7). Long-term $^{14}\text{CO}_2$ measurements exist at both site and regional fossil fuel CO_2 estimates are derived from these data in Levin et al. (2008). Analogous to the observations, the regional FFCO₂ offset at each station was determined for the simulations using Jungfraujoch high mountain station (Switzerland) as background reference level.

15 At SCH the observed mean regional fossil fuel CO_2 component is 1.5 ppm in 2002 and shows no significant seasonal cycle (Fig. 9). The simulation results of all transport models using the “IER_hourly” emissions show a large spread (Fig. 9, left panel) with annual mean values between 1.4 and 2.9 ppm and root mean square deviations from observations ranging from 0.5 to 1.6 ppm. The differences caused by the emission inventories, on the other hand, are significantly smaller (less than 0.5 ppm) than the deviations from the observations. This is illustrated in the left panel of Fig. 9 for REMO simulations using the different emission inventories.

25 A quantitative evaluation of the transport model performances using ^{14}C -based fossil fuel CO_2 observations is difficult because of compensating effects between transport model deficiencies, spatial resolution, and emission errors. For instance, LMDZ simulations show relatively good agreement with the ^{14}C data despite the coarse horizontal and vertical resolution of the model. On the other hand, high resolution models, which are more sensitive to the exact location of emission sources in the vicinity of a station, and which presumably better resolve transport characteristics, tend

to deviate more. This is even more obvious at the Heidelberg urban site, where the the REMO simulations are almost twice the ^{14}C -based fossil fuel CO_2 observation (Fig. S7, supplementary material: <http://www.atmos-chem-phys-discuss.net/9/7457/2009/acpd-9-7457-2009-supplement.pdf>). The spread between all transport model simulations at Heidelberg is also larger than the deviations from the observations. There is also a clear seasonal cycle at this station both in the observations and the model simulations. While the coarse resolution models are generally not very sensitive to differences between FFCO_2 emission maps, even at a polluted site, the high-resolution models show a clear improvement of the seasonal cycle at HEI if the inventory includes temporal variability. This result opens for further applications of the ^{14}C approach.

4 Impact on inversion of ecosystem fluxes

In this section we investigate the significance of the differences between the fossil fuel emission maps by quantifying their impact in the optimized biospheric fluxes. We compare the inverted ecosystem fluxes (F_{bio}) from different inversions for 2001, using the four different fossil fuel emission maps. Figure 10 presents the inversion-derived F_{bio} fluxes, expressed as deviations from the “EDG_annual” inversion, taken as a “reference”. We chose a constant FFCO_2 flux for the reference since this represents the commonly applied assumption in global inverse modelling. We first discuss the mean of F_{bio} over Europe and then spatial differences (Fig. 10).

For all inversions, the monthly European F_{bio} flux shows a large seasonal cycle (as expected) with a maximum carbon uptake in June (not shown). The amplitude of the seasonal cycle is in the order of 1 Gt C/month integrated over Europe ($12 \cdot 10^6 \text{ km}^2$). Differences between fossil fuel maps induces F_{bio} differences of less than 0.04 Gt C/month , which is very small compared to the seasonal cycle and much lower than the estimated Bayesian uncertainty returned by the inversions (in the order of 0.1 Gt C/month). Logically, accounting for temporal variations in the fossil fuel emissions

Fossil CO_2 model intercomparison

P. Peylin et al.

Title Page

Abstract

Introduction

Conclusions

References

Tables

Figures

◀

▶

◀

▶

Back

Close

Full Screen / Esc

Printer-friendly Version

Interactive Discussion



**Fossil CO₂ model
intercomparison**

P. Peylin et al.

[Title Page](#)[Abstract](#)[Introduction](#)[Conclusions](#)[References](#)[Tables](#)[Figures](#)[◀](#)[▶](#)[◀](#)[▶](#)[Back](#)[Close](#)[Full Screen / Esc](#)[Printer-friendly Version](#)[Interactive Discussion](#)

(“EDG_hourly” versus “EDG_annual”) decreases the estimated biosphere flux in winter and increases it during summer, as a compensation for the seasonality imposed on the fossil fuel emissions (“EDG_hourly”). If we consider smaller regions, like the “western part” of Europe, the differences remain similar. The impact of the temporal variations of fossil fuel emissions on the derived monthly Fbio fluxes remain below 5%. These results are consistent across the two inverse set ups (LMDz and TM3).

Integrated over the year, the inversion-derived Fbio differences become much more significant than on the monthly time scale (Table 5). Although the effect of accounting for temporal variations in fossil fuel emissions (“EDG_hourly” versus “EDG_annual”) on the Fbio estimates is limited to less than 5% (integrated over Europe or its “Western part”), the effect of switching emission patterns and magnitudes lead to much larger differences. For instance, using “IER_hourly” emission map changes the mean value of Fbio by ~ 0.15 Gt C/yr for the whole Europe and by ~ 0.05 Gt C/yr for the Western part. These numbers are slightly smaller than the annual differences in fossil fuel emission (0.23 Gt C/yr for Europe, Table 2) because part of the fossil fuel difference is compensated by Fbio (and Focean) flux adjustments outside Europe. The use of the “T3_annual” emissions induces smaller changes (less than 20% integrated over Europe). Overall, it should be realized that the largest fossil difference corresponds to 30–40% of the annual Fbio for Europe estimated for that particular year (2001). Note that the two inversion-derived annual Fbio fluxes for Europe are of the same magnitudes than the mean fluxes estimated by Janssens et al. (2003).

To focuss on the spatial flux distribution over Europe, Fig. 10 illustrates for July the impact of fossil fuel emission maps on the estimated Fbio spatial distribution. We compare the results using “EDG_annual” (reference case, bottom panel) to the differences between using “IER_hourly” and “EDG_annual” (top panel). For this particular month, the differences obtained with the “LMDz” and “TM3” inversions appear to be on the order of 2 to 6 g C/m²/month across a large part of Europe (with maximum values close to 10 g C/m²/month) while the reference Fbio shows carbon uptake between 20 and 100 g C/m²/month in the same area. On a country

**Fossil CO₂ model
intercomparison**

P. Peylin et al.

Title Page

Abstract

Introduction

Conclusions

References

Tables

Figures

◀

▶

◀

▶

Back

Close

Full Screen / Esc

Printer-friendly Version

Interactive Discussion



scale, a change of fossil fuel emission map could thus significantly affect the Fbio flux: for each country the averaged impact can reach 20% in July. If the same diagnostic is applied to annual Fbio larger differences are found, as expected from the above analysis of Europe integrated fluxes. These Fbio differences can directly be compared to the differences between the emission maps themselves. The differences between “IER_hourly” and “EDG_annual” fossil fuel sources for July (Fig. S1, supplementary material: <http://www.atmos-chem-phys-discuss.net/9/7457/2009/acpd-9-7457-2009-supplement.pdf>) can reach $\pm 100 \text{ g C/m}^2/\text{month}$ over industrial areas (i.e., Western Germany). This result confirms that the inversions tend to smooth these large FFCO₂ emission differences and distribute them spatially over adjacent regions.

These results hold for all months and reflect the under-constrained nature of current inversions. Overall these sensitivity tests highlight the increasing impact of uncertainties (mainly biases) in fossil fuel emission maps on the estimated biosphere fluxes from the continental to the regional scale.

5 Discussion: transport versus FFCO₂ emission errors

We have shown the impact of differences in current fossil fuel emission maps on modeled FFCO₂ concentrations at European stations and further assessed the impact on two state of the art atmospheric inversions. In Sect. 3.1 it was demonstrated that the atmospheric transport model differences have a substantially larger impact on FFCO₂ concentrations than the differences between emission maps. To investigate this issue further, we calculated the mean concentration field and the corresponding standard deviation (std-dev) when varying either the emissions or the atmospheric transport. The results, analysed for January and July, at 12:00 local time (Fig. 11) clearly confirms the findings from Sect. 3.1. Standard deviation from the transport models (σ_{trsp} , left panels) are substantially larger than std-dev from the emissions (σ_{emis} , right panels), both in January and in July.

**Fossil CO₂ model
intercomparison**

P. Peylin et al.

[Title Page](#)[Abstract](#)[Introduction](#)[Conclusions](#)[References](#)[Tables](#)[Figures](#)[I◀](#)[▶I](#)[◀](#)[▶](#)[Back](#)[Close](#)[Full Screen / Esc](#)[Printer-friendly Version](#)[Interactive Discussion](#)

Moreover, the std-dev are larger in winter compared to the summer, due to enhanced wintertime trapping of the emissions. Away from large emission sources, σ_{emis} and σ_{trsp} are rather small, although the transport models show considerable disagreement over the Atlantic Ocean in summer ($\sigma_{\text{trsp}} \sim 1$ ppm). This is linked to large differences in PBL mixing and wind fields between the models in summer. Interestingly, the largest variability among the transport models is not always found just over the emission areas, but for instance over the Alps, where σ_{trsp} reaches up to 8 ppm in winter. Obviously, high resolution models resolve the emission, orography, and the associated transport patterns better than coarse resolution models, an effect that was also observed in Fig. 8. Concerning σ_{emis} , the largest variability appears in areas with large emissions (see Fig. 1). It is indeed at these locations that the emission inventories differ in their spatial and temporal patterns. Depending on the location, the ratio between σ_{trsp} and σ_{emis} varies between 2 and 8 (larger model differences) with maximum ratios in January.

If we now consider the station locations where current CO₂ measurements take place, Table 6 compares σ_{trsp} and σ_{emis} computed for the whole year using hourly or monthly mean values. For the sites that are currently used in most atmospheric inversion (HUN, Mace Head (MHD), Schauinsland (SCH), Monte Cimone (CMN)) the hourly FFCO₂ spread caused by the transport model differences (between 1 and 2 ppm) appears to be ~ 3 times larger than the spread caused by the emission maps. Using monthly mean concentrations reduce the difference to a factor 2.5, with σ_{trsp} and σ_{emis} around 0.7 ppm and 0.3 ppm, respectively. These numbers indicate that although transport model uncertainties dominate over Europe, differences in annual fossil fuel estimates or neglecting their temporal variations also play a critical role. If we now consider stations that are closer to anthropogenic emission areas, like Black Sea Coast (BSC) and Saclay (SAC) near Paris, the ratio between transport model spread and emission spread becomes on the order of two or even less. The assimilation of observed concentrations at these sites would increase the sensitivity of inverse modeling-derived biosphere fluxes to fossil fuel uncertainties.

6 Conclusions

We analyzed the importance of differences between fossil-fuel CO₂ emission inventories and the importance of sub-annual variations in these emissions for tracer transport modelling and regional scale inverse modelling of the European C-cycle, by testing four alternative fossil fuel mpas. Although the fossil-fuel emission is often considered as the “well known” term in the terrestrial carbon balance, annual differences between emission inventories are typically ~10% at the country level reaching up to 40% for some European countries. These differences increase with decreasing length scale, and correspond to systematic errors due to inconsistent accounting systems (i.e. see for instance Ciais et al., 2008). Seasonal and diurnal variations in fossil fuel emissions, which are commonly neglected, reach amplitudes close to 40% and 80%, respectively.

The significance of these emission differences for inverse modelling depends on how they relate to other sources of uncertainty. We have investigated their relative importance in comparison with transport model uncertainties, which also adresses the question whether fossil fuel CO₂ could be used as a diagnostic tracer for testing atmospheric transport or if atmospheric CO₂ inversions would rather inform us about fossil fuel CO₂ emissions. The impact of the fossil-fuel emission uncertainties on modeled FFCO₂ concentrations at the European stations is on the order of 0.4 ppm (std-dev calculated with the same model but different emissions) while the impact of using several transport models with the same emission is 2–3 times larger, depending on the location and period of the year. We additionally quantified the impact of fossil fuel uncertainties on two state of the art inversions. Monthly changes in estimated biosphere fluxes at the European scale are small and less than 4% but annual changes become critical, as expected from the differences in annual emission totals. Differences up to 0.15 Gt C/yr are of similar magnitude as the total European carbon sink estimated by Janssens et al. (2003).

These results indicate that uncertainties in fossil fuel emission inventories cannot be ignored in applications of inverse modelling of the European C-cycle, and that in order

Fossil CO₂ model intercomparison

P. Peylin et al.

Title Page

Abstract

Introduction

Conclusions

References

Tables

Figures

◀

▶

◀

▶

Back

Close

Full Screen / Esc

Printer-friendly Version

Interactive Discussion



to advance our understanding of the net carbon exchange of the European terrestrial biosphere, the consistency of the European fossil fuel inventories needs substantial improvement. Not only the national and annual scales but also finer spatial and temporal scales need to be improved to aid regional modelling studies. Sub-annual FFCO₂ emission variations lead to significant changes in the seasonal and diurnal concentration variations at the European stations of up to few ppm (~2 ppm at HUN).

We have used emission maps for one particular year (2000) but there is a need for similar high-resolution inventories for subsequent years to account for changing emissions associated to the economic development and for CO₂ emissions that are dependant on the meteorological conditions such as domestic heating. Within the North American Carbon Project (NACP), the “VULCAN” project (<http://www.purdue.edu/eas/carbon/vulcan/index.php>) is going in this direction with a recent release of a new emission map for North America at hourly time scale on a 10 km grid. Several efforts are also ongoing in Europe within EDGAR and IER groups but also within national agencies. These efforts need to be continued, harmonized, and validated at several levels of the data processing chain. For example, the IER emission inventory used in this study is much more precise for Germany than for other countries, which can lead to systematic FFCO₂ concentration differences between stations and induce critical biases in the inversion results.

Finally, monitoring of fossil fuel CO₂ is in principle possible with radiocarbon (¹⁴CO₂) measurements in the PBL over the continent (Levin et al., 2003). Currently ¹⁴CO₂ is measured quasi-continuously only at very few stations in Europe and mostly integrated over time periods of one or several weeks. From first comparisons of the model simulations with monthly ¹⁴C-based fossil fuel CO₂ observations it was not yet possible to discriminate between the four FFCO₂ emission maps. Moreover, the large differences between simulated and observed FFCO₂ call for a further systematic evaluation of the transport characteristics in the models. High-resolution time series of FFCO₂, which are based on a combination of hourly CO measurements with weekly-integrated ¹⁴CO₂ measurements (Levin and Karstens, 2007), will become available at several stations

**Fossil CO₂ model
intercomparison**

P. Peylin et al.

Title Page

Abstract

Introduction

Conclusions

References

Tables

Figures

◀

▶

◀

▶

Back

Close

Full Screen / Esc

Printer-friendly Version

Interactive Discussion



and will allow a more detailed analysis of diurnal to synoptic scale differences. Overall, improvements of the transport models are clearly needed before an independent verification of emission inventories through comparisons of simulated and observed fossil fuel CO₂ might become feasible.

- 5 *Acknowledgements.* We thank the research group of IER for the construction of a detailed European fossil fuel emission map, within the CarboEurope Integrated Program (CE-IP). CE-IP also partly funded this work and resources for the different simulations. We also thank Ingeborg Levin for providing the monthly-integrated fossil fuel CO₂ based on ¹⁴CO₂ observations available in the CarboEurope database.

10



The publication of this article is financed by CNRS-INSU.

References

- 15 Baker, D. F., Law, R. M., Gurney, K. R., Rayner, P., Peylin, P., Denning, A. S., Bousquet, P., Bruhwiler, L., Chen, Y.-H., Ciais, P., Fung, I. Y., Heimann, M., John, J., Maki, T., Maksyutov, S., Masarie, K., Prather, M., Pak, B., Taguchi, S., and Zhu, Z.: TransCom 3 inversion inter-comparison: Impact of transport model errors on the interannual variability of regional CO₂ fluxes, 1988–2003, *Global Biogeochem. Cycles*, 20, GB1002, doi:10.1029/2004GB002439, 2006. 7465
- 20 Bousquet, P., Peylin, P., Ciais, P., Quere, C. L., Friedlingstein, P., and Tans, P. P.: Regional changes in carbon dioxide fluxes of land and oceans since 1980, *Science*, 290, 1342–1346, 2000. 7465
- Brenkert, A. L.: Carbon Dioxide Emission Estimates from Fossil-Fuel Burning, Hydraulic Cement Production, and Gas Flaring for 1995 on a One Degree Grid Cell Basis, Document

7483

ACPD

9, 7457–7503, 2009

Fossil CO₂ model intercomparison

P. Peylin et al.

Title Page

Abstract

Introduction

Conclusions

References

Tables

Figures

◀

▶

◀

▶

Back

Close

Full Screen / Esc

Printer-friendly Version

Interactive Discussion



file for database NDP-058a 2-1998, Oak Ridge National Laboratory, Oak Ridge, Tennessee, 1998. 7462, 7487

Canadell, J. G., Le Quere, C., Raupach, M. R., Field, C. B., Buitenhuis, E. T., Ciais, P., Conway, T. J., Gillett, N. P., Houghton, R. A., and Marland, G.: Contributions to accelerating atmospheric CO₂ growth from economic activity, carbon intensity, and efficiency of natural sinks, *Proceedings of the National Academy of Sciences of the United States of America*, 104, 18866–18870, doi:10.1073/pnas.0702737104, 2007. 7460

Ciais, P., Paris, J., Marland, G., Peylin, P., Piao, S., Levin, I., Pregger, T., Scholz, Y., Friedrich, R., Houwelling, S., and Schulze, D.: The European carbon balance revisited. Part 4: fossil fuel emissions, *Global Biogeochem. Cycles*, in review, 2008. 7465, 7481

Denning, A. S., Fung, I., and Randall, D.: Latitudinal gradient of atmospheric CO₂ due to seasonal exchange with land biota, *Nature*, 376, 240–243, 1995. 7461

Geels, C., Christensen, J. H., Frohn, L. M., and Brandt, J.: Simulating spatiotemporal variations of atmospheric CO₂ using a nested hemispheric model, *Phys. Chem. Earth*, 27, 1495–1506, 2002. 7489

Geels, C., Gloor, M., Ciais, P., Bousquet, P., Peylin, P., Vermeulen, A. T., Dargaville, R., Aalto, T., Brandt, J., Christensen, J. H., Frohn, L. M., Haszpra, L., Karstens, U., Rödenbeck, C., Ramonet, M., Carboni, G., and Santaguida, R.: Comparing atmospheric transport models for future regional inversions over Europe – Part 1: mapping the atmospheric CO₂ signals, *Atmos. Chem. Phys.*, 7, 3461–3479, 2007, <http://www.atmos-chem-phys.net/7/3461/2007/>. 7467, 7470

Gurney, K., Chen, Y., Maki, T., Kawa, S., Andrews, A., and Zhu, Z.: Sensitivity of atmospheric CO₂ inversions to seasonal and interannual variations in fossil fuel emissions, *J. Geophys. Res.-Atmos.*, 110, D10308, doi:10.1029/2004JD005373, 2005. 7460, 7461

Gurney, K. R., Law, R. M., Denning, A. S., et al.: Towards robust regional estimates of CO₂ sources and sinks using atmospheric transport models, *Nature*, 415, 626–630, 2002. 7468

Hauglustaine, D. A., Hourdin, F., Jourdain, L., Filiberti, M.-A., Walters, S., Lamarque, J.-F., and Holland, E. A.: Interactive chemistry in the Laboratoire de Météorologie Dynamique general circulation model: Description and background tropospheric chemistry evaluation, *J. Geophys. Res.*, 109, D04314, doi:10.1029/2003JD003957, 2004. 7489

Heimann, M. and Körner, S.: The global atmospheric tracer model TM3, Model description and user's manual Release 3.8a, Max Planck Institute of Biogeochemistry, 2003. 7489

Janssens, I., Freibauer, A., Ciais, P., Smith, P., Nabuurs, G., Folberth, G., Schlamadinger,

**Fossil CO₂ model
intercomparison**

P. Peylin et al.

Title Page

Abstract

Introduction

Conclusions

References

Tables

Figures

◀

▶

◀

▶

Back

Close

Full Screen / Esc

Printer-friendly Version

Interactive Discussion



**Fossil CO₂ model
intercomparison**

P. Peylin et al.

[Title Page](#)[Abstract](#)[Introduction](#)[Conclusions](#)[References](#)[Tables](#)[Figures](#)[◀](#)[▶](#)[◀](#)[▶](#)[Back](#)[Close](#)[Full Screen / Esc](#)[Printer-friendly Version](#)[Interactive Discussion](#)

B., Hutjes, R., Ceulemans, R., Schulze, E., Valentini, R., and Dolman, A.: Europe's terrestrial biosphere absorbs 7 to 12% of European anthropogenic CO₂ emissions, *Science*, 300, 1538–1542, doi:10.1126/science.108592, 2003. 7478, 7481

Keeling, C. D., Bacastow, R. B., Carter, A. F., Piper, S. C., Whorf, T. P., Heimann, M., Mook, W. G., and Roeloffzen, H. A.: A three-dimensional model of atmospheric CO₂ transport based on observed winds: 1. Analysis of observational data, in: *Aspects of climate variability in the Pacific and the Western Americas*, Geophysical monograph 55, edited by: Peterson, D. H., pp. 165–236, AGU, 1989. 7472

Krol, M., Houweling, S., Bregman, B., van den Broek, M., Segers, A., van Velthoven, P., Peters, W., Dentener, F., and Bergamaschi, P.: The two-way nested global chemistry-transport zoom model TM5: algorithm and applications, *Atmos. Chem. Phys.*, 5, 417–432, 2005, <http://www.atmos-chem-phys.net/5/417/2005/>. 7489

Langmann, B.: Numerical modelling of regional scale transport and photochemistry directly together with meteorological processes, *Atmos. Environ.*, 34, 3585–3598, 2000. 7489

Law, R. M., Peters, W., Rödenbeck, C., et al.: TRANSCOM model simulations of hourly CO₂: experimental overview and diurnal results for 2002, *Global Biogeochem. Cycles*, 22, GB3009, doi:10.1029/2007GB003050, 2007. 7462, 7467, 7468, 7487

Levin, I. and Karstens, U.: Inferring high-resolution fossil fuel CO₂ records at continental sites from combined (CO₂)-C-14 and CO observations, *Tellus Series B-Chemical and Physical Meteorology*, 59, 245–250, doi:10.1111/j.1600-0889.2006.00244.x, 2007. 7482

Levin, I., Kromer, B., Schmidt, M., and Sartorius, H.: A novel approach for independent budgeting of fossil fuel CO₂ over Europe by ¹⁴CO₂ observations, *Geophys. Res. Lett.*, 30, 2194, doi:10.1029/2003GL018477, 2003. 7475, 7482

Levin, I., Hammer, S., Kromer, B., and Meinhardt, F.: Radiocarbon observations in atmospheric CO₂: Determining fossil fuel CO₂ over Europe using Jungfraujoch observations as background, *Sci. Total Environ.*, 391, 211–216, doi:10.1016/j.scitotenv.2007.10.019, 2008. 7476

Marland, G., Boden, T. A., and Andres, R. J.: Global, Regional, and National Fossil Fuel CO₂ Emissions, in: *Trends: A Compendium of Data on Global Change*, US department of energy, Carbon Dioxide Information Analysis Center, Oak Ridge National Laboratory, Oak Ridge, Tenn., USA, 2006. 7465

Peylin, P., Rayner, P. J., Bousquet, P., Carouge, C., Hourdin, F., Heinrich, P., Ciais, P., and AEROCARB contributors: Daily CO₂ flux estimates over Europe from continuous atmospheric measurements: 1, inverse methodology, *Atmos. Chem. Phys.*, 5, 3173–3186, 2005,

<http://www.atmos-chem-phys.net/5/3173/2005/>. 7468

Pregger, T., Scholz, Y., and Friedrich, R.: Documentation of the anthropogenic GHG emission data for Europe provided in the Frame of CarboEurope GHG and CarboEurope IP, Project report, Institut für Energiewirtschaft und Rationelle Energieanwendung, Universität Stuttgart, Stuttgart, Germany, 2007. 7463, 7464, 7487

Rödenbeck, C., Houweling, S., Gloor, M., and Heimann, M.: CO₂ flux history 1982–2001 inferred from atmospheric data using a global inversion of atmospheric transport, *Atmos. Chem. Phys.*, 3, 1919–1964, 2003, <http://www.atmos-chem-phys.net/3/1919/2003/>. 7465, 7468

Schmidt, H., Derognat, C., Vautard, R., and Beekmann, M.: A comparison of simulated and observed ozone mixing ratios for the summer of 1998 in Western Europe, *Atmos. Environ.*, 36, 6277–6297, 2001. 7489

Stephens, B. B., Gurney, K. R., Tans, P. P., Sweeney, C., Peters, W., Bruhwiler, L., Ciais, P., Ramonet, M., Bousquet, P., Nakazawa, T., Aoki, S., Machida, T., Inoue, G., Vinnichenko, N., Lloyd, J., Jordan, A., Heimann, M., Shibistova, O., Langenfelds, R. L., Steele, L. P., Francey, R. J., and Denning, A. S.: Weak northern and strong tropical land carbon uptake from vertical profiles of atmospheric CO₂, *Science*, 316, 1732–1735, doi:10.1126/science.1137004, 2007. 7468

Stohl, A., Eckhardt, S., Forster, C., James, P., and Spichtinger, N.: On the pathways and timescales of intercontinental air pollution transport, *J. Geophys. Res.-Atmos.*, 107, doi:10.1029/2001JD001396, 2002. 7475

van Aardenne, J. A., Dentener, F. J., Olivier, J. G. J., Peters, J. A. H. W., and Ganzeveld, L. N.: The EDGAR 3.2 Fast track 2000 dataset (32FT2000), Tech. rep., Joint Research Centre (JRC), Ispra, Italy, available from <http://www.mnp.nl/edgar/model/v32ft2000edgar>, 2005. 7463, 7487

Vermeulen, A. T., Pieterse, G., Hensen, A., van den Bulk, W. C. M., and Erisman, J. W.: COMET: a Lagrangian transport model for greenhouse gas emission estimation – forward model technique and performance for methane, *Atmos. Chem. Phys. Discuss.*, 6, 8727–8779, 2006, <http://www.atmos-chem-phys-discuss.net/6/8727/2006/>. 7489

Vestreng, V., Breivik, K., Adams, M., Wagener, A., Goodwin, J., Rozovskkaya, O., and Pacyna, J. M.: Inventory Review 2005, Emission Data reported to LRTAP Convention and NEC Directive, Initial review of HMs and POPs, MSC-W 1/2005 ISSN 0804-2446, EMEP, 2005. 7463

**Fossil CO₂ model
intercomparison**

P. Peylin et al.

Title Page

Abstract

Introduction

Conclusions

References

Tables

Figures

◀

▶

◀

▶

Back

Close

Full Screen / Esc

Printer-friendly Version

Interactive Discussion



Fossil CO₂ model intercomparison

P. Peylin et al.

Table 1. Tracer definition.

Tracer name	Inventory	Time variation	Hor. Resolution	Ref.
Transcom3	CDIAC NDP-058A ^a	constant	1°×1°	Brenkert (1998)
EDGAR Annual	Edgar FT2000	constant	1°×1°	van Aardenne et al. (2005)
EDGAR Hourly	Edgar FT2000	hourly ^b	1°×1°	van Aardenne et al. (2005)
IER Hourly	IER inventory	hourly	10×10 km ² – 1°×1° ^c	Pregger et al. (2007)

^a Gridded data were prepared for the Transcom Continuous Experiment (Law et al., 2007).

^b Mean temporal profiles were used, representing average European conditions (provided by EMEP).

^c <1°×1° for Europe only; 10×10 km² over Germany.

Title Page

Abstract

Introduction

Conclusions

References

Tables

Figures

◀

▶

◀

▶

Back

Close

Full Screen / Esc

Printer-friendly Version

Interactive Discussion



Fossil CO₂ model intercomparison

P. Peylin et al.

Table 2. Comparison of annual fossil fuel emission estimates for the year 2000.

Country	EDGAR FT2000 Pg C	IER Pg C	Marland Pg C	Max-Min (%)
Germany	0.262	0.234	0.224	15
France	0.119	0.111	0.099	18
Italy	0.130	0.126	0.122	6
Spain	0.089	0.084	0.082	8
England	0.162	0.148	0.154	9
Netherlands	0.057	0.047	0.039	38
Europe	1.989	1.752	–	13

Title Page

Abstract

Introduction

Conclusions

References

Tables

Figures

◀

▶

◀

▶

Back

Close

Full Screen / Esc

Printer-friendly Version

Interactive Discussion



Fossil CO₂ model
intercomparison

P. Peylin et al.

Table 3. Overview of participating atmospheric transport models.

Model	Domain	Horizontal Resolution	Vertical levels	Meteorology	Ref.
LMDZ	global	3.75° × 3.75°	19 η	ECMWF	Hauglustaine et al. (2004)
TM3	global	4° × 5°	19 σ	NCEP	Heimann and Körner (2003)
TM5	global	3° × 2°	25 η	ECMWF	Krol et al. (2005)
	Europe	1° × 1°			Krol et al. (2005)
DEHM	Europe	0.5° × 0.5°	20 σ	ECMWF/MM5	Geels et al. (2002)
REMO	Europe	0.5° × 0.5°	20 η	ECMWF	Langmann (2000)
CHIMERE	Europe	0.5° × 0.5°	20 σ up to 500 hPa	ECMWF/MM5	Schmidt et al. (2001)
COMET	Lagrangian	– ^a	2 ^b	ECMWF	Vermeulen et al. (2006)

^a Trajectories calculation from meteorological fields at 1° × 1°.^b Layer boundary at dynamically calculated PBL height.

Title Page

Abstract

Introduction

Conclusions

References

Tables

Figures

I◀

▶I

◀

▶

Back

Close

Full Screen / Esc

Printer-friendly Version

Interactive Discussion



Fossil CO₂ model intercomparison

P. Peylin et al.

Title Page

Abstract

Introduction

Conclusions

References

Tables

Figures

◀

▶

◀

▶

Back

Close

Full Screen / Esc

Printer-friendly Version

Interactive Discussion



Table 4. Set up of the two inversions.

	LMDz inversion	TM3 inversion
Flux resolution	Monthly×Pixel based	Weekly×Pixel based
Observations	70 sites; Monthly data	70 sites×Flask data
Prior fluxes	Biosphere model (ORCHIDEE)	No prior model
Prior errors	Based on NPP + spatial correlations	based on distance

Fossil CO₂ model intercomparison

P. Peylin et al.

Table 5. Inverse fluxes in Gt C/yr with Edgar annual fossil fuel estimated and inverse flux differences with the 3 other fossil fuel estimates.

	Flux using	Flux differences		
	Edgar_ann	Edgar_hr - Edgar_ann	IER_hr – Edgar_ann	Transcom – Edgar_ann
LMDZ Tot Europe	–0.35	–0.01	0.14	0.06
LMDZ West Europe	–0.03	–0.00	0.05	0.02
TM3 Tot Europe	–0.57	0.01	0.15	0.11
TM3 West Europe	–0.41	0.00	0.03	0.01

[Title Page](#)
[Abstract](#)
[Introduction](#)
[Conclusions](#)
[References](#)
[Tables](#)
[Figures](#)
[Back](#)
[Close](#)
[Full Screen / Esc](#)
[Printer-friendly Version](#)
[Interactive Discussion](#)


Fossil CO₂ model intercomparison

P. Peylin et al.

Table 6. Annual averaged standard deviation of Hourly/monthly averaged fossil fuel CO₂ concentrations (ppm) at a few stations for the whole year. Standard deviations were calculated either for the mean CO₂ emission tracer across the transport models, or for the mean transport model across the CO₂ emission tracers.

station	Transport Hourly/Monthly	Tracer Hourly/Monthly
BSC	0.99/0.58	0.50/0.46
CMN	1.07/0.90	0.23/0.22
HUN115	1.46/0.94	0.59/0.51
MHD	0.75/0.52	0.24/0.22
SCH	1.13/0.73	0.35/0.29
SAC	2.34/1.69	1.16/1.07

[Title Page](#)
[Abstract](#)
[Introduction](#)
[Conclusions](#)
[References](#)
[Tables](#)
[Figures](#)
[I◀](#)
[▶I](#)
[◀](#)
[▶](#)
[Back](#)
[Close](#)
[Full Screen / Esc](#)
[Printer-friendly Version](#)
[Interactive Discussion](#)


**Fossil CO₂ model
intercomparison**

P. Peylin et al.

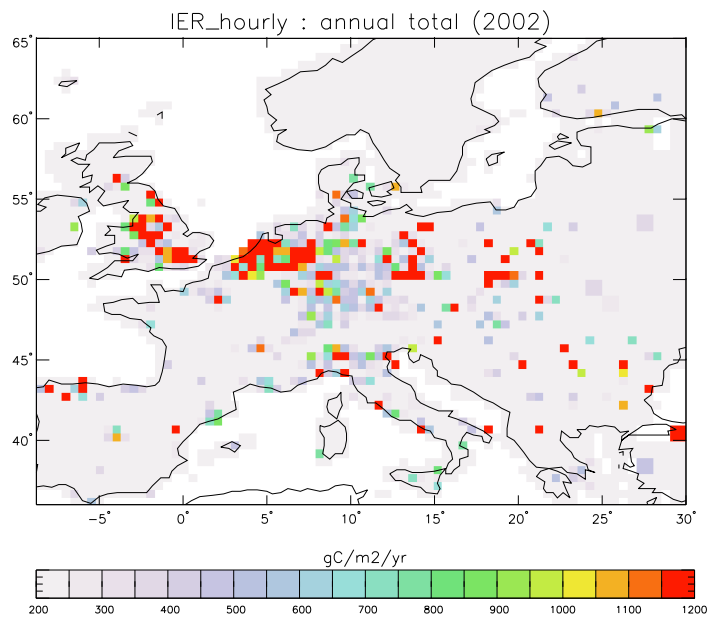


Fig. 1. Annual fossil fuel emissions from the “IER_hourly” inventory.

[Title Page](#)[Abstract](#)[Introduction](#)[Conclusions](#)[References](#)[Tables](#)[Figures](#)[I◀](#)[▶I](#)[◀](#)[▶](#)[Back](#)[Close](#)[Full Screen / Esc](#)[Printer-friendly Version](#)[Interactive Discussion](#)

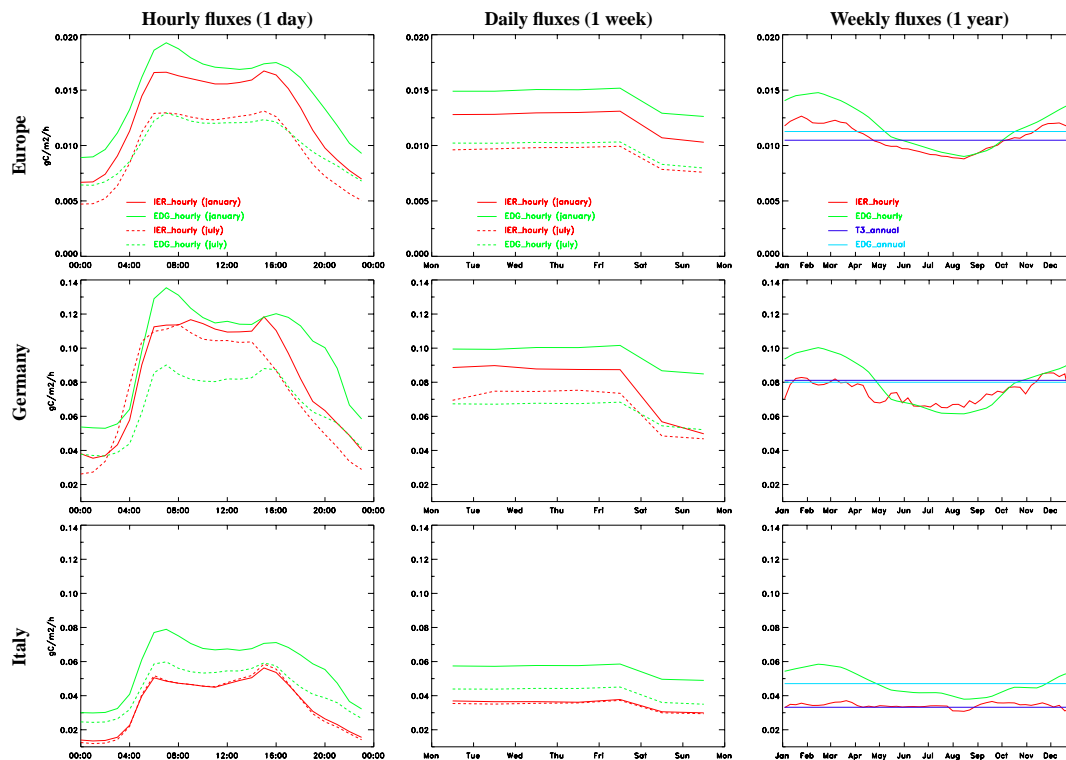


Fig. 2. Temporal variation of the aggregated fluxes over different regions: Europe (top), Germany (middle) and Italy (bottom). First and second columns represent the mean diurnal cycle and the mean weekly cycle, respectively, for “IER_hourly” and “EDG_hourly” in July and January; Third column represents the seasonal variations (weekly means) for the four emissions maps. Note that the y-range is different for Europe (much smaller).

[Title Page](#)
[Abstract](#)
[Introduction](#)
[Conclusions](#)
[References](#)
[Tables](#)
[Figures](#)
[◀](#)
[▶](#)
[◀](#)
[▶](#)
[Back](#)
[Close](#)
[Full Screen / Esc](#)
[Printer-friendly Version](#)
[Interactive Discussion](#)


Fossil CO₂ model
intercomparison

P. Peylin et al.

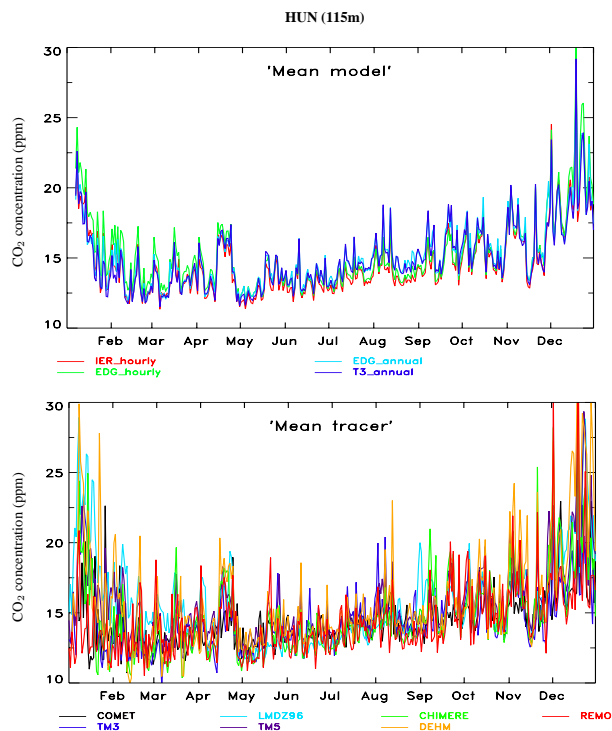


Fig. 3. Day-time mean simulated FFCO₂ concentration at the Hungarian tall tower (HUN): mean across all transport models for each emission map (top) and mean across all emission map for each transport model (bottom).

[Title Page](#)[Abstract](#)[Introduction](#)[Conclusions](#)[References](#)[Tables](#)[Figures](#)[◀](#)[▶](#)[◀](#)[▶](#)[Back](#)[Close](#)[Full Screen / Esc](#)[Printer-friendly Version](#)[Interactive Discussion](#)

Fossil CO₂ model
intercomparison

P. Peylin et al.

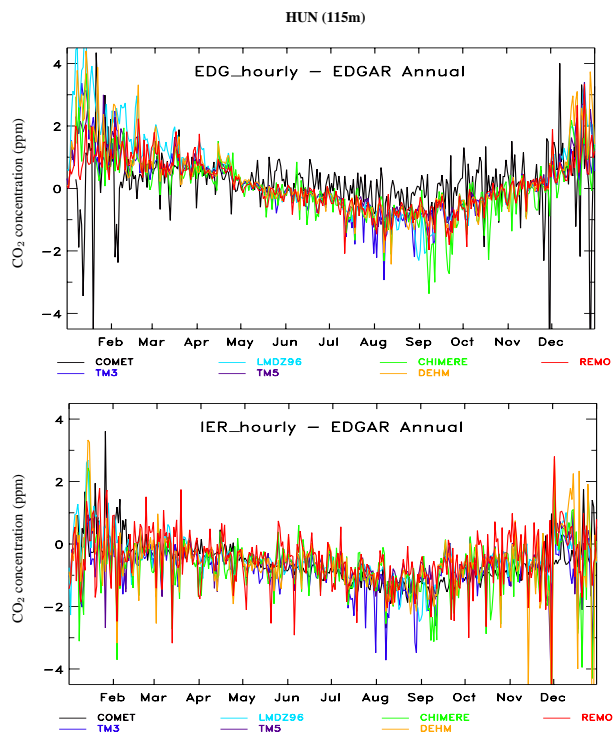


Fig. 4. Day-time mean simulated FFCO₂ concentration difference at HUN between “EDG_hourly” and “EDG_annual” fluxes (top) and between “IER_hourly” and “EDG_annual” fluxes (bottom).

[Title Page](#)[Abstract](#)[Introduction](#)[Conclusions](#)[References](#)[Tables](#)[Figures](#)[◀](#)[▶](#)[◀](#)[▶](#)[Back](#)[Close](#)[Full Screen / Esc](#)[Printer-friendly Version](#)[Interactive Discussion](#)

Fossil CO₂ model
intercomparison

P. Peylin et al.

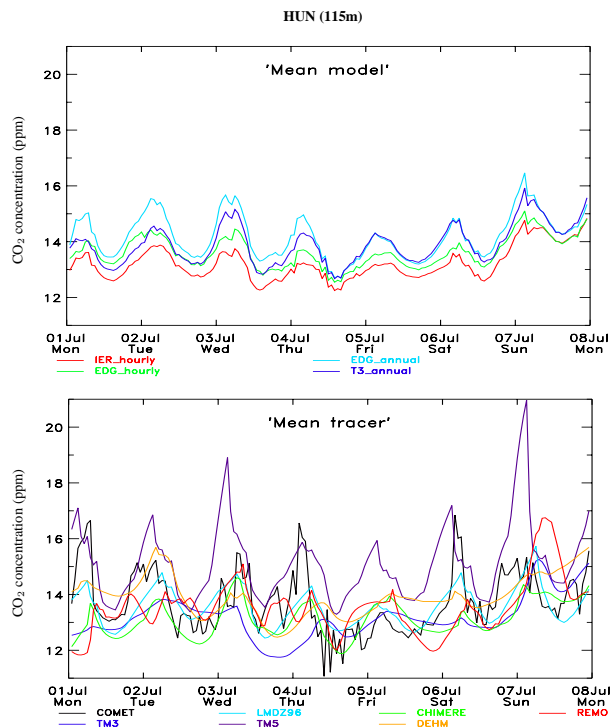


Fig. 5. Hourly simulated concentrations at HUN for 1 week in July: top: Mean across all transport models for each emission map; bottom: Mean across all emission maps for each transport model.

[Title Page](#)[Abstract](#)[Introduction](#)[Conclusions](#)[References](#)[Tables](#)[Figures](#)[◀](#)[▶](#)[◀](#)[▶](#)[Back](#)[Close](#)[Full Screen / Esc](#)[Printer-friendly Version](#)[Interactive Discussion](#)

Fossil CO₂ model
intercomparison

P. Peylin et al.

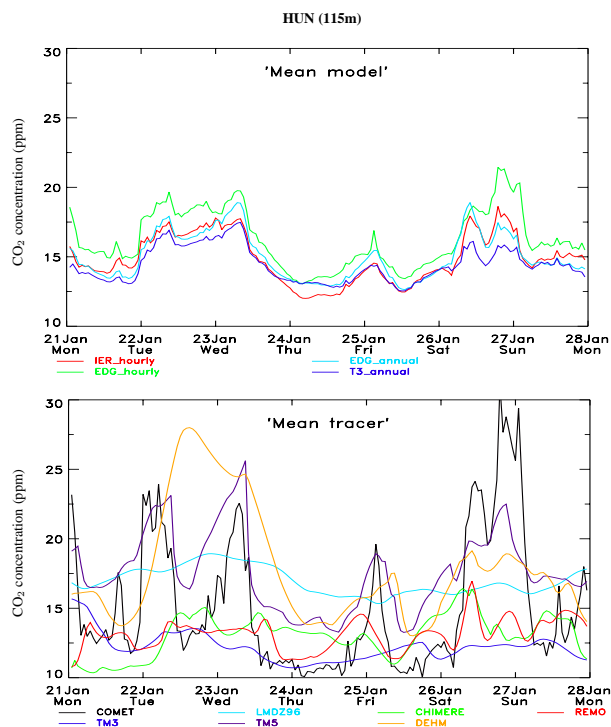


Fig. 6. Hourly simulated concentrations at HUN for 1 week in January. Top: Mean across all models for each tracer; Bottom: Mean across all tracer for each model.

[Title Page](#)[Abstract](#)[Introduction](#)[Conclusions](#)[References](#)[Tables](#)[Figures](#)[◀](#)[▶](#)[◀](#)[▶](#)[Back](#)[Close](#)[Full Screen / Esc](#)[Printer-friendly Version](#)[Interactive Discussion](#)

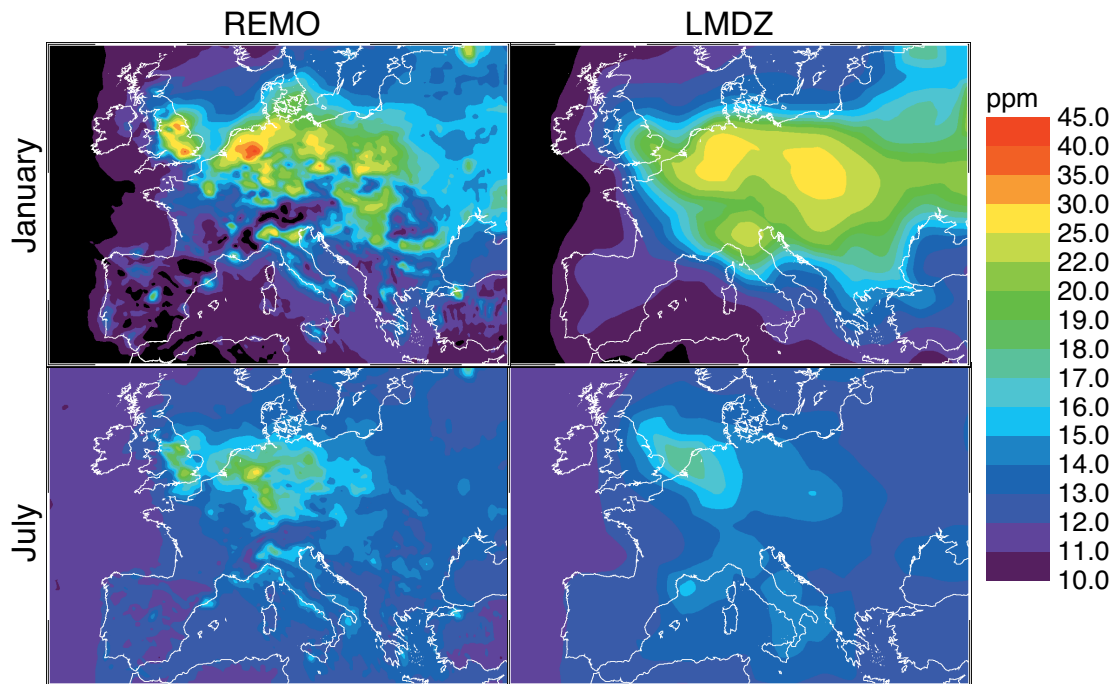


Fig. 7. Comparison of fossil fuel CO₂ fields as calculated by the highest (REMO) and the lowest resolution model (LMDZ) included in the inter-comparison, using “IER_hourly” emission map. The numbers represent monthly averaged surface concentrations sampled at 12:00 local time. The surface layer is defined as 0–150 m above the ground.

Fossil CO₂ model intercomparison

P. Peylin et al.

Title Page

Abstract

Introduction

Conclusions

References

Tables

Figures

◀

▶

◀

▶

Back

Close

Full Screen / Esc

Printer-friendly Version

Interactive Discussion



Fossil CO₂ model
intercomparison

P. Peylin et al.

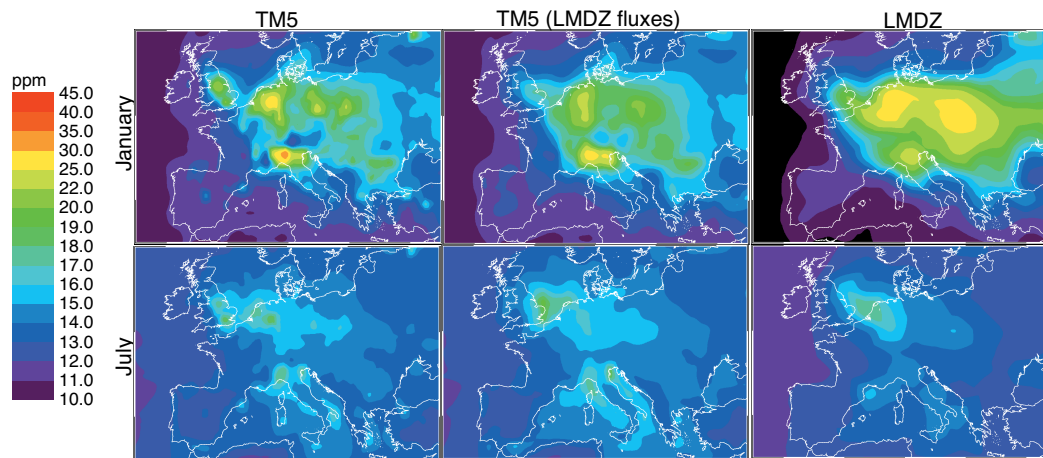


Fig. 8. Comparison of TM5, LMDZ, and TM5 with fossil fuel CO₂ emissions added on the LMDZ resolution. For further details see caption Fig. 7.

[Title Page](#)[Abstract](#)[Introduction](#)[Conclusions](#)[References](#)[Tables](#)[Figures](#)[◀](#)[▶](#)[◀](#)[▶](#)[Back](#)[Close](#)[Full Screen / Esc](#)[Printer-friendly Version](#)[Interactive Discussion](#)

Fossil CO₂ model
intercomparison

P. Peylin et al.

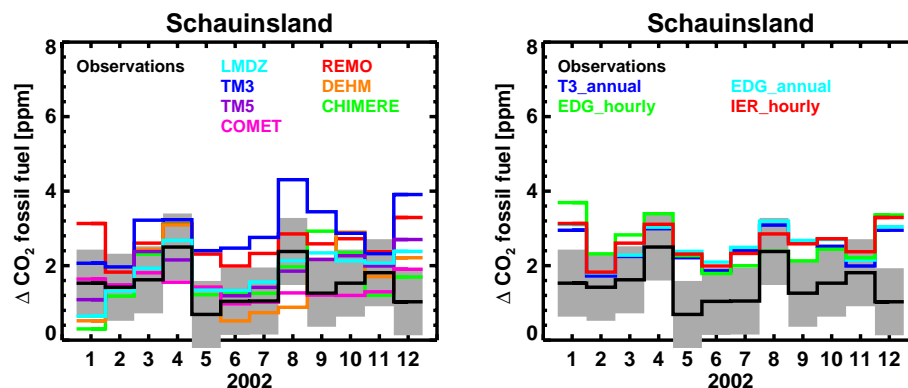


Fig. 9. Comparison of monthly-integrated fossil fuel CO₂ (relative to Jungfraujoch) at Schauinsland based on ¹⁴CO₂ observations with simulations of all transport models using the “IER_hourly” emission map (left panel) and with simulations of the regional model REMO using the four different emission maps (right panel). An uncertainty estimate of observed monthly mean fossil fuel CO₂ is included (grey shading).

[Title Page](#)[Abstract](#)[Introduction](#)[Conclusions](#)[References](#)[Tables](#)[Figures](#)[◀](#)[▶](#)[◀](#)[▶](#)[Back](#)[Close](#)[Full Screen / Esc](#)[Printer-friendly Version](#)[Interactive Discussion](#)

Fossil CO₂ model
intercomparison

P. Peylin et al.

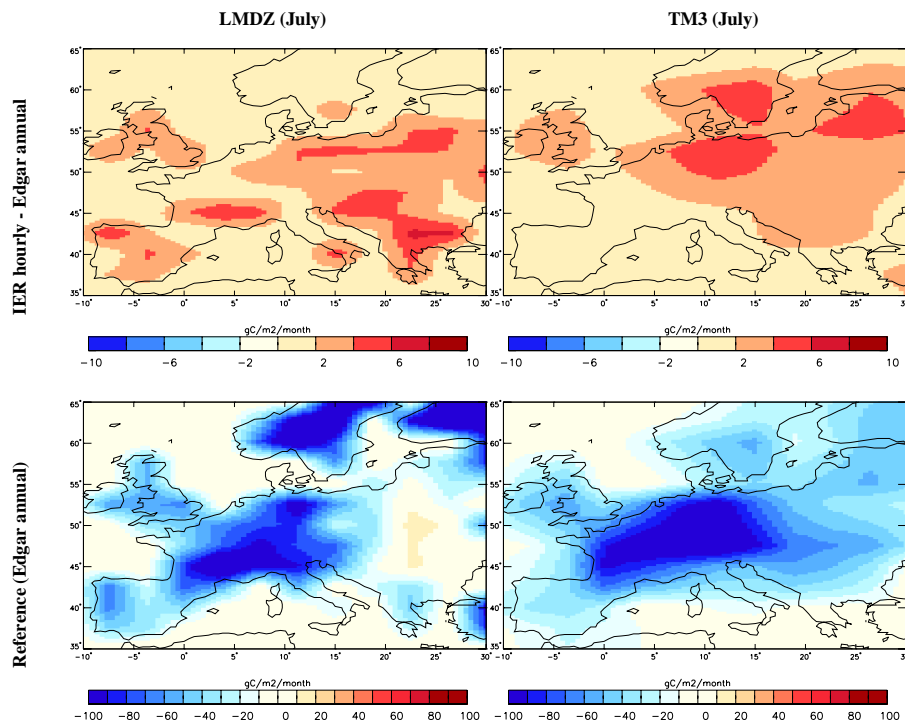


Fig. 10. July biosphere fluxes estimated with the LMDZ and TM3 inversions (see text for methodology) for a case using “EDG_annual” fossil fuel emissions (lower panels) and the difference between using “IER_hourly” and “EDG_annual” emissions (upper panels).

[Title Page](#)[Abstract](#)[Introduction](#)[Conclusions](#)[References](#)[Tables](#)[Figures](#)[◀](#)[▶](#)[◀](#)[▶](#)[Back](#)[Close](#)[Full Screen / Esc](#)[Printer-friendly Version](#)[Interactive Discussion](#)

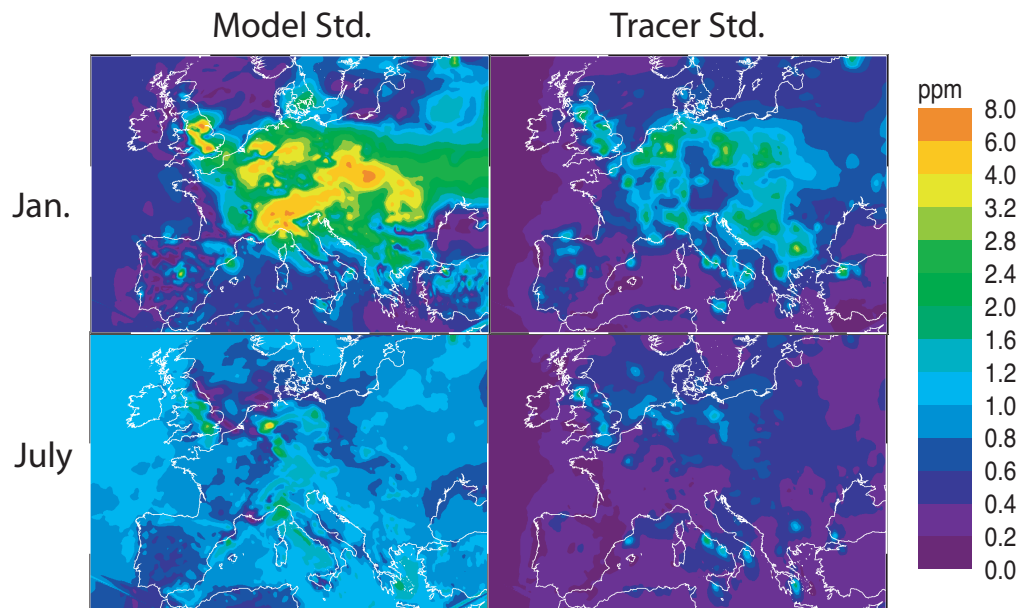


Fig. 11. Standard deviation of monthly averaged fossil fuel CO₂ concentrations. Standard deviations are calculated either for the mean FFCO₂ emission inventories across the transport models (left), or for the mean transport model across the FFCO₂ emission inventories (right). Monthly mean averaged surface concentrations are calculated as in Fig. 7.

Fossil CO₂ model intercomparison

P. Peylin et al.

Title Page

Abstract

Introduction

Conclusions

References

Tables

Figures

◀

▶

◀

▶

Back

Close

Full Screen / Esc

Printer-friendly Version

Interactive Discussion

